AD-A073 497 ISRAEL INST OF METALS HAIFA F/G 11/6
ELECTRONMICROSCOPIC STUDY OF SAND EROSION PROCESSES IN METALS.(U)
JUN 79 J ZAHAVI AFOSR-78-3580
UNCLASSIFIED 041152 EOARD-TR-79-5 NL

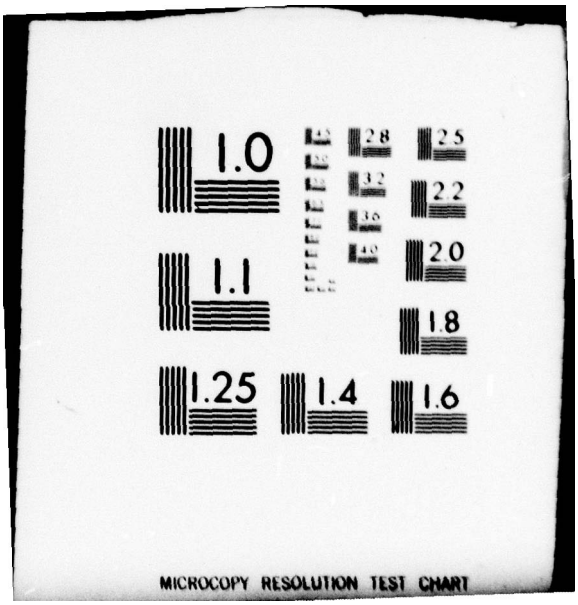
1.0
1.1
1.25
1.4
1.6
2.0
2.2
2.5
1.8
MICROCOPY RESOLUTION TEST CHART

MINISTRY OF INDUSTRY, COMMERCE AND TOURISM
INDUSTRIAL RESEARCH ADMINISTRATION

ISRAEL INSTITUTE OF METALS מכון המתכות הישראלי

TECHNION RESEARCH AND DEVELOPMENT FOUNDATION LTD

(2) LEVEL II

Electronmicroscopic Study of Sand Erosion Processes in Metals

Dr J. ZAHAVI

Grant Number AFOSR-78-3580

ELECTRONMICROSCOPIC STUDY OF SAND EROSION PROCESSES IN METALS

Joseph Zahavi

Israel Institute of Metals

Technion - Israel Institute of Technology

Haifa, Israel

JUNE 1979

Final Scientific Report 1 March 1978 - 28 February 1979

Approved for public release:
distribution unlimited

Prepared for
European Office of Aerospace Research & Development
London, England.

REPORT DOCUMENTATION PAGE		READ INSTRUCTIONS BEFORE COMPLETING FORM
1. Report Number EOARD-TR-79-5	2. Govt Accession No.	3. Recipient's Catalog Number
4. Title (and Subtitle) ELECTRONMICROSCOPIC STUDY OF SAND EROSION PROCESSES IN METALS.		5. Type of Report & Period Covered Final Scientific Report. 1 Mar 78 - 28 Feb 79.
		6. Performing Org. Report Number 041 152
7. Author(s) Dr. Joseph Zahavi		8. Contract or Grant Number AFOSR-78-3582
9. Performing Organization Name and Address Israel Institute of Metals, Technion R&D Foundation Technion Haifa, Israel		10. Program Element, Project, Task Area & Work Unit Numbers PE 61102F Proj Task 2301-01 68
11. Controlling Office Name and Address European Office of Aerospace Research and Development, Box 14 FPO New York 09510		12. Report Date JUN 1979 13. Number of Pages 32
14. Monitoring Agency Name and Address		15. Unclassified

16. & 17. Distribution Statement

Approved for public release; distribution unlimited.

18. Supplementary Notes Composite alloys were prepared in cooperation with Prof. R. Merhalrian, Dept of Metallurgy, Univ. of Illinois, Ill. 61801, USA. Technical assistance of Mr. S. Feinberg, Israel Inst. of Metals, is very much appreciated.

19. Key Words

Erosion, composite aluminium alloy, abrasive sand particles, eroded surface

20. Abstract

Knowledge and understanding of the variables, both environmental and metallurgical, affecting erosion of materials, are detrimental to predicting erosion behavior and ~~to take steps in~~ minimizing erosion damage.

In this study erosion behavior of composite aluminium alloys containing hard phase constituents such as silicon carbides and alumina has been investigated. Use has been made of electron microscopy techniques for →

393 650 JOB

79 08 24 062

FORM 1473

examination of eroded surface morphology, structure and composition with special attention to the effect of hard phase particles on erosion processes i.e. material removal.

It has been found that higher fraction of hard particles in metal alloy led to higher target weight loss under the same erosion conditions.

Observations of eroded surface obtained by SEM suggest that erosion process or material removal is composed of two basic processes:

a. local material removal from particle-free surface target.

b. complete removal of hard particles from the eroded target surface.

The behavior of composite metal alloys should be further investigated to gain more information and understanding of the role of hard phase constituents on erosion process? in composite metal alloys should be investigated further.

393650

EOARD-TR-79-5

20 August 1979

This report has been reviewed by the Information Office (EOARD/CMI) and is releasable to the National Technical Information Service (NTIS). At NTIS it will be releasable to the general public, including foreign nations.

This technical report has been reviewed and is approved for publication.

John T. Milton

JOHN T. MILTON
Scientific and Technical Information Officer

Gordon L. Hermann

GORDON L. HERMANN
Lt Colonel, USAF
Chief, Structures and Materials

FOR THE COMMANDER

Gordon L Hermann

GORDON L. HERMANN
Lt Colonel, USAF
Deputy Commander

CONTENTS

		Page
1.	Introduction	1
2.	Background	1
3.	Experimental	2
3.1	Alloys preparation	2
3.1.1	Materials	3
3.1.2	Procedure	3
3.1.3	Specimens and surface treatment	4
3.2	Erosion system	5
3.2.1	Apparatus	5
3.2.2	Abrasive sand particles	5
3.2.3	Erosion Tests	5
3.2.4	Microscopy Examination	6
4.	Results and Discussion	6
4.1	Erosion Behavior	6
4.1.1	Effect of composition alloy	6
4.1.2	Effect of impact angle	7
4.2	Target Surface Characterization	8
4.2.1	General Appearance	8
4.2.2	Local Erosion Processes and Hard Phase Particles.	9
5.	Further Discussion	10

1. INTRODUCTION

The first report dealt primarily with the preparation of aluminium composite alloys containing alumina and silicon carbide hard phases and their behavior under various erosion conditions. In this annual report we shall summarize the work described in the first report as well as describe further results concerning microscopy of target specimens regarding surface morphology, structure and composition before and after being exposed to various erosion conditions.

The help and advice of Professor R. Merhalrian in preparing the composite aluminium alloy specimens at his casting laboratory, Department of Metallurgy, University of Illinois, Urbana, Ill. U.S.A., is very much appreciated.

2. BACKGROUND

The erosion of ductile materials by a stream of abrasive particles has been a subject of practical importance in the operation of aircraft engines in sandy or dusty environments. Papers on the subject began appearing about 1960 and reflected the interest of the National Gas Turbine Establishment in England[1-5], and gas turbine engine manufacturers in the U.S.A.[6]. These papers were largely aimed at quantifying the effect of the engineering parameters, such as impingement velocity, impact angle, particle size, and target material, on the erosion rate. At the same time these works considered the mechanisms of metal removal by hard particles and presented results of electron microscope investigation of morphological changes that occurred.

The subject has also been approached from an engineering mechanics viewpoint[7, 8] and valuable insight into the erosion processes has been gained. Details of the microscopic deformation and removal process has also been presented for erosion of ductile metals by steel balls[9].

In a recent investigation[10] the correlation of surface morphology with sand erosion rate of ductile metallic materials i.e. Ti-6Al-4V, SS. 410 and 2024T4 Al has been studied. The results obtained showed that sand erosion process was the result of two separate processes occurring simultaneously, an intrinsic erosion process that removes metal and an adhesion process that embeds sand particles in the surface.

Examination of the eroded surfaces with a scanning electron microscope and an electron probe microanalyzer revealed that sand fragments became embedded in the metal surfaces and that the intrinsic erosion process was the result of a sequence of more localized material removal processes occurring when the metal surface was struck by the sand particles.

These local erosion processes were characterized by undermining around hard microconstituents and by cratering. The size of these microconstituents (aluminium rich phases in Ti-6Al-4V and iron or copper-rich phases in 2024 Al) about 10 microns was of the same order as the embedded particles and the cratered structure formed.

The aim of this research was to gain additional understanding of the mechanism of local material removal from eroded composite metallic surface containing hard phase particles by means of direct observation of surface morphology structure and composition in T.E.M., S.E.M. and E.P.M.

3. EXPERIMENTAL

3.1 Alloys preparation

Aluminium composite alloys containing hard phases of alumina and silicon carbide particles were produced for this investigation.

3.1.1 Materials

In this work commercially aluminium-copper alloy (Al 2024 - T4) made by Alcoa was utilized for preparation of aluminium composite alloy containing alumina and silicon carbide particles.

The incorporated alumina material particles was Alcoa Type A-10 in the sieved size of -140 mesh + 200 mesh.

The incorporated silicon carbide material particles was in the sieved sizes:

+ 100	mesh	917 gr.
- 100 + 140	mesh	1347 gr.
- 140 + 200	mesh	253 gr.
- 200	mesh	7 gr.

3.1.2 Procedure

The fabrication processes of the composite aluminium alloys were conducted together with Prof. R. Merhabrian, making use of his casting facilities at the University of Illinois, Urbana, Ill., U.S.A.

The preparation procedure consisted of the following stages:

a) Melting the Al 2024 - T4 alloy in an induction furnace.

b) Transferring the melt to a mullite-graphite crucible insite a resistance heated furnace with a carbon double blade stirrer.

c) Cooling the melt by continuous flow of argon until the temperature reaches the desired value in the liquid-solid zone.

d) Upon formation of solid particles of aluminium in the melt alumina or silicon carbide particles were fed into the melt.

e) The material was reheated above its liquidous temperature while agitation was continued.

f) The melt then was cast through a bottom hole into pre-heated 1" diameter and 5" long of graphite molds.

g) Thereafter the ingots were melted and squeezed cast under 6 ton load at 300°C to form pore free ingots in the size of 2" in diameter and 1.5" length.

3.1.3 Specimens and Surface Treatment

Specimens 2" in diameter and ¼" in thickness were cut with diamond saws from the prepared ingots of aluminium composite alloys.

The various kinds of specimens prepared for examination under erosion conditions in this work are listed below:

Type of Material	Matrix	Hard phase	Amount of phases	Heat treatment
Composite Aluminium Alloy	Al 2024	SiC	15% Vol. 30% Vol. 40-50% Vol.	As Casted
		Al_2O_3	15% Vol. 30% Vol.	
Aluminium Alloy	2024	-	-	T3
				To

Specimens prepared from non-composite 2024 aluminium alloys were squares in the size of 5x5x1 mm.

Specimens made of composite aluminium alloy were mechanically polished with 600 grit SiC paper and then with diamond compound on napless paper to provide uniformly smooth surfaces before being exposed to erosion conditions. Chemical treatment of these specimens would result in non-uniform surface. On the other hand samples made of Al 2024 To and Al 2024 T3

sheets were chemically polished in acid solutions containing H_2SO_4, H_3PO_4, HNO_3 (3 : 16 : 1) before erosion.

3.2 Erosion System

3.2.1 Apparatus

An air-blast sand erosion rig was used. Fig. 2 shows the principal elements of the rig. Filtered compressed air at room temperature is partially by-passed through a sand reservoir from which the sand is picked up and introduced into the main stream through a control orifice. The air-sand stream then flows through a 4:1 converging nozzle into the specimen chamber.

The air flow rate was measured with an orifice flow meter. The actual mean velocity of the sand entering the specimen chamber was measured by the time-of-flight device suggested by Ruff and Ives[11]. The device was inserted in place of the specimen chamber and calibrated against the nominal air flow rate, which was subsequently used for control. In the air velocity range used, the sand velociety proved to be about one-third the air velocity, (in agreement with the results of Ruff and Ives) shown in Fig. 2.

3.2.2 Abrasive Sand Particles

Natural sand collected from the shore of the Mediterranean Sea was sieved into the range of 210 to 297 μm and oven dried. This sand contained about 96 per cent by weight of SiO_2, the constituent considered to be responsible for its erosiveness. The grains were slightly rounded and somewhat elongated, as seen in Fig. 3.

3.2.3 Erosion Tests

The sand reservoir was filled with sand in amounts varying between 50 and 600 gr and the experimental run continued until all the sand had been exhausted from the reservoir. The max-

imum air velocity used was 150 m/sec, and the specimen impact angles were $\pi/2$, $\pi/3$, and $\pi/6$ rad (90^{o}, 60^{o}, and 30^{o}). Two to three runs were made for each experimental condition of air velocity, impingement angle, sand quantity, and alloy. Before and after exposure the specimens were weighed to 0.1 mg on an analytical balance.

3.2.4 Microscopy Examination

Optical and electron microscopy techniques were used in characterizing target surface before and after being exposed to erosion conditions. Electron probe microanalyzer (EPM) and a scanning microscopy together with an X-ray unit were used to correlate surface morphology and composition with erosion kinetics and presence of hard phases.

4. RESULTS AND DISCUSSION

The work carried out in this investigation aimed at studying erosion kinetics and erosion processes, i.e. material removal and how these were affected by the presence of hard phases embedded in the alloy matrix. The results obtained are described as follows:

4.1 Erosion Behavior

Figs. 4 and 5 show the relationships between target weight change and impingement angle of impacted erosive sand particles for aluminium alloy containing silicon carbide particles (Fig. 4), and alumina particles (Fig. 5). A constant amount of 500 gr. sand particles struck target surfaces at 42 m/sec for the kinetic data shown in Figs. 4 and 5.

4.1.1 Effect of Alloy Composition

Target weight loss vs. impact angle curves shown in Fig. 4 suggested that increasing the amount of SiC particles in the aluminium matrix resulted in higher target weight loss when exposed to erosive conditions at a given impact angle.

In eroded aluminium alloy containing 15% SiC weight loss was about 25% to 50% more compared to free particle alloy while in eroded aluminium alloy containing 40-50% SiC weight loss measured was about 5-6 times compared to non-composite alloy (Fig. 4).

In observing the behavior of aluminium alloy containing various amounts of alumina particles under erosive conditions as shown in Fig. 5, it can be deduced that the higher the amount of alumina particles the higher was the weight loss measured. The behavior of these composite aluminium alloys under erosive conditions can be explained by the fact that besides local material removal processes occurring at matrix surface the hard phase particles either SiC or Alumina are removed completely from target surface. That particles were removed from the eroded target surface was also confirmed by microscopy examination (see 4.2).

4.1.2 Effect of Impact Angle

Composite aluminium alloy specimens containing 15% or less by volume of hard phase particles, either SiC or alumina, showed maximum weight loss at low impact angles of 30° and minimum weight loss at normal angles as shown in Figs. 4 and 5. This behavior is typical for ductile materials being exposed to impact of abrasive particles[10].

Increasing the amount of hard phases in the matrix (up to 30% in volume) led to maximum target weight loss at impact angle of 60° as can be seen in Figs. 4 and 5 for SiC and Alumina particles respectively.

Furthermore, increasing the amount of SiC up to 40-50% (volume) in the matrix led to independence of target weight loss on impact angle (Fig. 4). This can be explained by assuming that at such high concentration of hard phase particles in the alloy matrix (40-50% SiC in 2024 Al) target

weight loss is governed primarily by removal of complete particles from target surface. Removal of particle from the surface is not affected very much by the abrasive particles impacted angle.

4.2 Target Surface Characterization

4.2.1 General Appearance

Optical Microscopy - A typical general appearance of composite aluminium alloy containing silicon carbide particles as observed with optical microscope is shown in Fig. 6. Before being exposed to erosion conditions the surface contained uniformly distributed silicon carbide particles 100 to 150 microns in size with angular shape as can be seen in Fig. 6A. The particles appear in the photographs (Fig. 6) as bright zones surrounded by dark rim. After erosion many of the hard silicon particles were removed leaving craters and grooves on target surface (dark zones in the photograph, Fig. 6). Removal of hard phase particles from eroded target surface was found at low impact angle (30^{o} see Fig. 6B) as well as at normal angle (90^{o}, Fig. 6C). Careful examination of the eroded surface revealed that some of the grooves or craters (dark areas in the photograph, Fig. 6) contain pieces or fragments of hard phase particles (bright spot areas within the dark zones) which might suggest that particle removal was associated with breaking or fracturing of the hard brittle particles. Detailed observations of target surface were conducted by making use of electron microscopy, and the results obtained are described herein.

Scanning Electron Microscopy - The general appearance of the surfaces as observed with the scanning electron microscope is shown in Figs. 7 to 10 for composite aluminium alloy containing silicon carbide particles and in Figs. 11, 12 for alumina particles.

Surface morphology of composite aluminium alloys containing silicon carbides and alumina before being exposed to various erosion conditions is shown in Fig. 7 (a to c) and in Fig. 11 (a, b) respectively.

Target surface as seen with the SEM before erosion is character-

ized by the presence of hard phase particles some of which are fully embedded in the surface, some are protruding at various angles from the surface and some are not at the surface any more, leaving craters at their traces (Fig. 7a). A typical silicon carbide particle, its shape and the way it is embedded in the target surface, as well as the interface between the particle and target matrix, is shown in Fig. 7b. X-ray pictures of Figs. 7c and 7d show the presence of Si(Kα) and Al (Kα) in the area shown in Fig. 7b.

After erosion all the composite aluminium alloys containing either silicon carbide or alumina particles exhibited a cratered structure independent of impact angle as shown in Figs. 7-10 for silicon carbide and in Figs. 11, 12 for alumina particles.

The crater structure (10 to 30 microns in size) is characteristic to eroded surface of ductile material such as aluminium as was observed in a previous work[10]. The general appearance of the eroded composite alloys surface is also characterized by the presence or absence of hard phase particles. These particles either remained unaffected by the impacted sand particles (Figs. 7, 9, 10, 11) or were removed completely from the surface, leaving some traces of fractured areas (Fig. 8, for example). The presence of hard phase particles in the alloy matrix did not affect the local erosion processes in free particle local areas in target surface.

4.2.2 Local Erosion Processes and Hard Phase Particles

The general cratered structure of eroded surfaces was the result of many localized material removal processes occurring when the metal surface was struck by the abrasive particles[10]. Localized material removal processes at free particle surface area resulted in cratered type structure in all the alloys examined. However, when abrasive sand struck directly on hard particle in the target surface no material removal or cratered structure was detected in the particle as can be seen in Figs. 9 and 10.

Furthermore when a particle was embedded just below the target surface it stopped the continuation of local material removal upon exposing the particle surface (Figs. 9, 10).

Upon exposing target surface to various erosion conditions some of the hard phase particles were removed completely from the surface (Fig. 8). The removal of the particle was associated with its breaking up or fracturing as shown in Figs. 8a-8d. Removal of the hard phase particles resulted in high weight loss or high erosion compared to non-composite alloy exposed under the same erosion condition as shown in Fig. 4.

Examination of eroded surface of aluminium alloy containing alumina particles showed that local material removal occurred around the particles (Figs. 11, 12) where the particles themselves were removed thereafter.

Local material removal was associated with breaking up of abrasive particles upon striking the surface and thereafter penetration of abrasive fragments into the surface, Figs. 8e and 8f. This was observed previously in ductile non-composite alloys of aluminium[10].

5. FURTHER DISCUSSION

Although it would be too early at this stage of the work to draw general conclusions on the behavior of composite metal alloys under erosive conditions and consequently on the mechanism by which material is removed, the results presented in this report provide additional knowledge for better understanding of the behavior of aluminium composite alloys (ASTM 2024 Al) containing high fractions of hard constituents such as silicon carbide and alumina.

The kinetic study, i.e. the weight change measurements (shown in Figs. 4 and 5) indicates that the greater the fraction or the amount of hard phase particles in the aluminium matrix the greater is target weight

loss under the same erosion conditions. These results strongly suggest that the presence of hard phase constituents in the matrix alloy has a detrimental effect on the erosion behavior and erosion damage.

The high rate of erosion measured in the composite aluminium alloys compared to non-composite aluminium alloys can be explained by assuming that sand erosion process in the composite alloys is composed of two processes: a) removal of material from the matrix free particle surface; b) removal of hard phase particles completely from the surface (Fig. 6).

The SEM study revealed that sand erosion process in composite aluminium alloys was the result of several material removal processes taking place at impacted target surface: a) local material removal from target surface resulted in cratered type structure 10 to 30 microns in size as can be seen in Figs. 7-12;

b) Removal of hard phase constituents and particles primarily by undermining of the material immediately next to these particles as shown, for example, in Figs. 8, 9 & 11. Removal of these particles from the surface resulted in a fractured surface containing fragments of the hard particle material for instance, silicon carbide as can be seen in Figs. 8a-8d.

c) Adhesion of abrasive fragment particles on the eroded surface. Embedded sand particles can be seen in Figs. 8e-8f. This process was found previously[10] on non-composite aluminium alloy.

Further work should be conducted in order to gain more understanding regarding the behavior of composite alloys under erosive conditions. However, on the basis of this work it is concluded that the higher the fraction of hard phase particles in the matrix alloy, the higher is the weight loss under sand erosion conditions and this should be taken into consideration when erosion resistance materials are concerned for various applications.

References

1) Tilly, G.P., Wear, Vol. 23, 1973, pp. 87-96.

2) Tilly, G.P. and Sage, W., Wear, Vol. 16, 1970, pp. 447-465.

3) Goodwin, J.E., Sage, W., and Tilly, G.P., Proceedings, The Institute of Mechanical Engs., Vol. 184, Part 1, No. 15, 1960-1970, pp. 279-292.

4) Tilly, G.P., Wear, Vol. 14, 1969, pp. 63-79.

5) Tilly, G.P., Wear, Vol. 14, 1969, pp. 241-248.

6) Smeltzer, C.E., Gulben, M.E. and Compton, W.A., Journal of Basic Engineering Transactions of the A.S.M.E., Sept. 1970, pp. 638-654.

7) Finnie, I., Wear, Vol. 19, 1972, pp. 81-90.

8) Finnie, I., Wolak, J., and Kabil, Y., Journal of Materials, Vol. 2, No. 3, Sept. 1967, pp. 682-700.

9) Hutchings, I.M. and Winter, R.W., Wear, Vol. 27, 1974, pp. 121-128.

10) Zahavi, J., Wagner, H.J. and A. Posnansky, "Characterization of the Damage introduced by Sand Erosion Processes in Metals", A.S.T.M. Symposium on "Erosion: Prevention and Useful Applications", October 24-26, 1977, Vail, Colorado, U.S.A.

11) Ruff, A.W. and Ives, L.K. Wear, Vol. 35, 1975, pp. 195-199.

APPENDIX

MICROGRAPHS

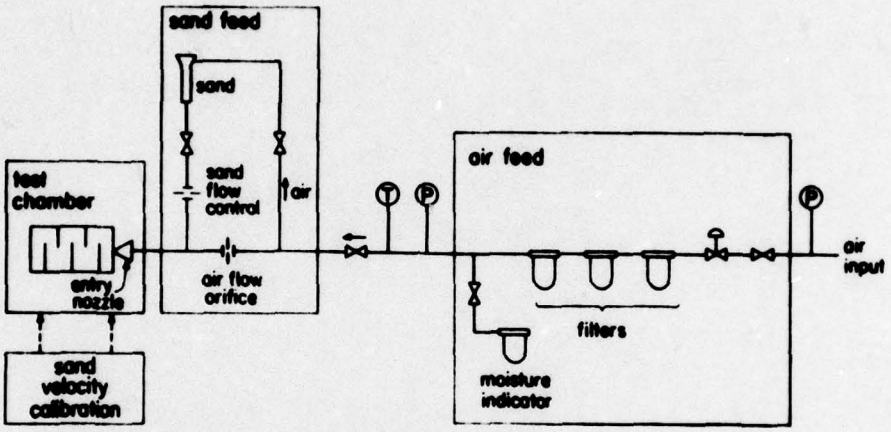

Fig. 1: Schematic of erosion experimental set up

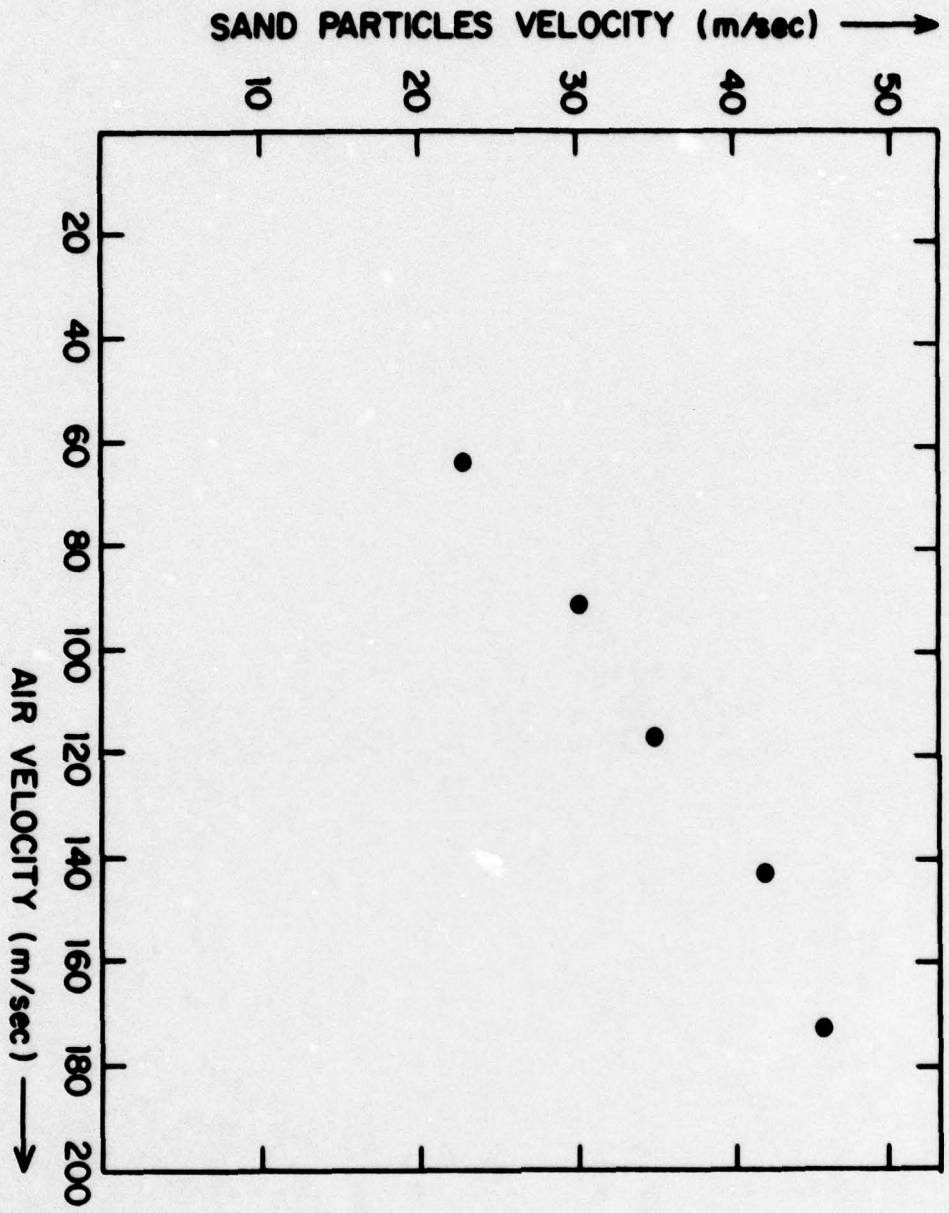

Fig. 2: Erosive sand particles velocity as function of air velocity in the erosion apparatures.

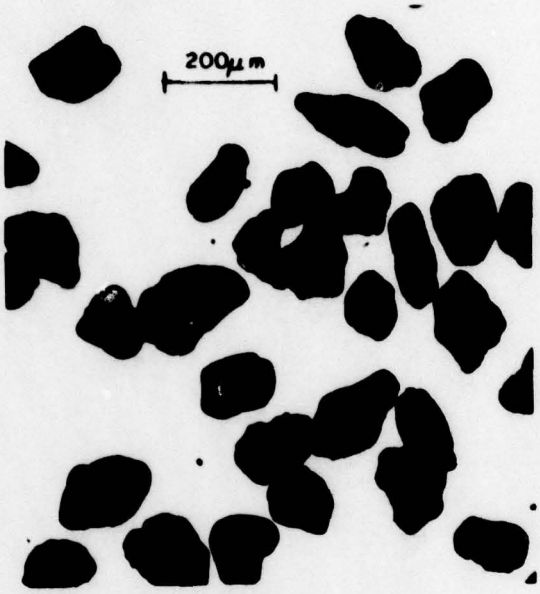

Fig. 3: Micrograph of erosive sand particles.

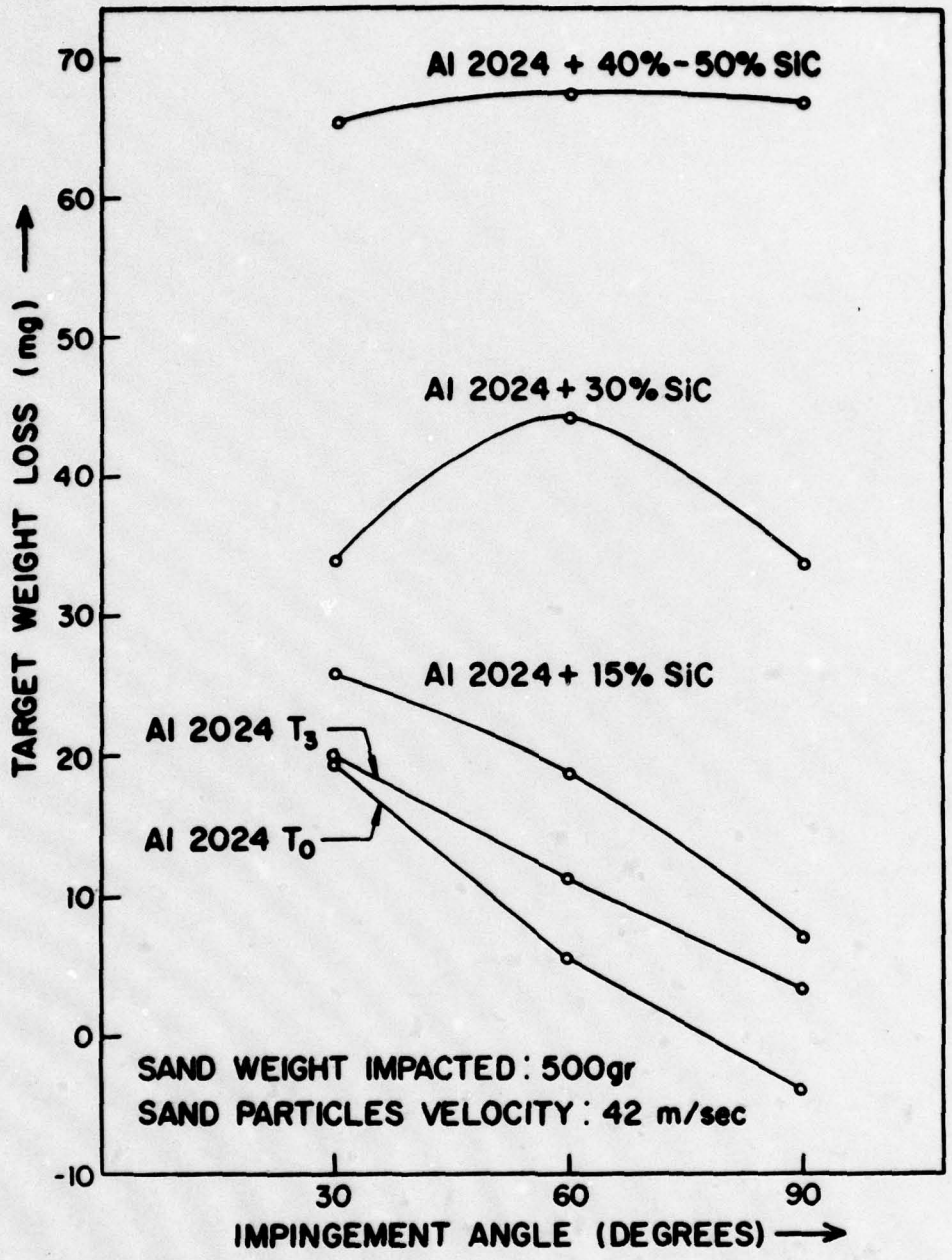

Fig. 4: Variation of Target Weight Change with Impingement Angles at Particles Impact Velocity of 42 m/sec (Specimens containing various amounts of SiC).

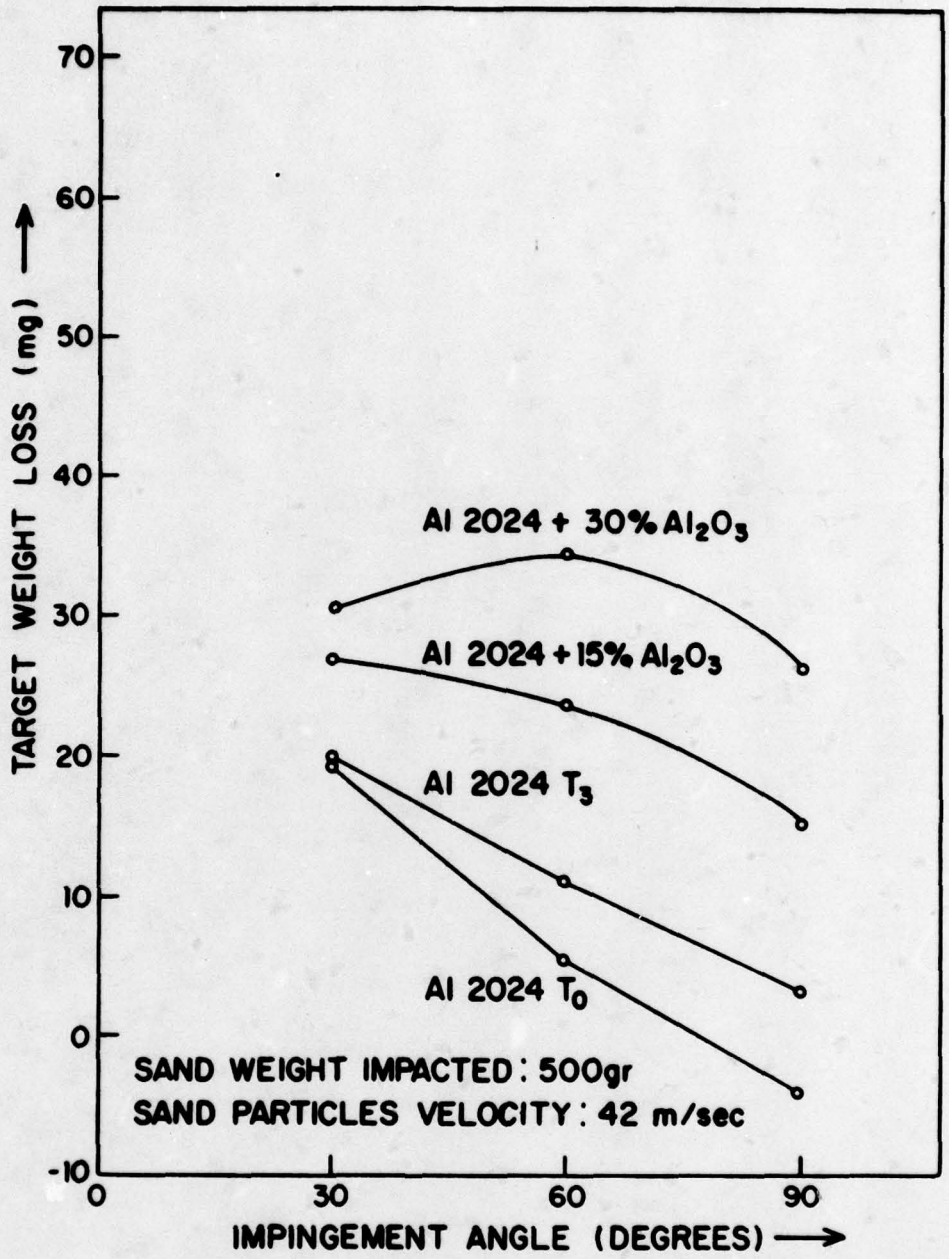

Fig. 5: Variation of Target Weight Change with Impingement Angle at Particles Impact Velocity of 42 m/sec. (Specimens containing various amounts of Al_2O_3).

Fig. 6; Optical micrographs of composite aluminium alloy specimens containing 30% Vol. silicon carbide particles

A. Surface appearance before erosion

B. Surface appearance after being eroded by 500 gr. sand particles at impact angle of 30^{o}.

C. Surface appearance after being eroded by 500 gr. sand particles at impact angle of 90^{o}.


A


B

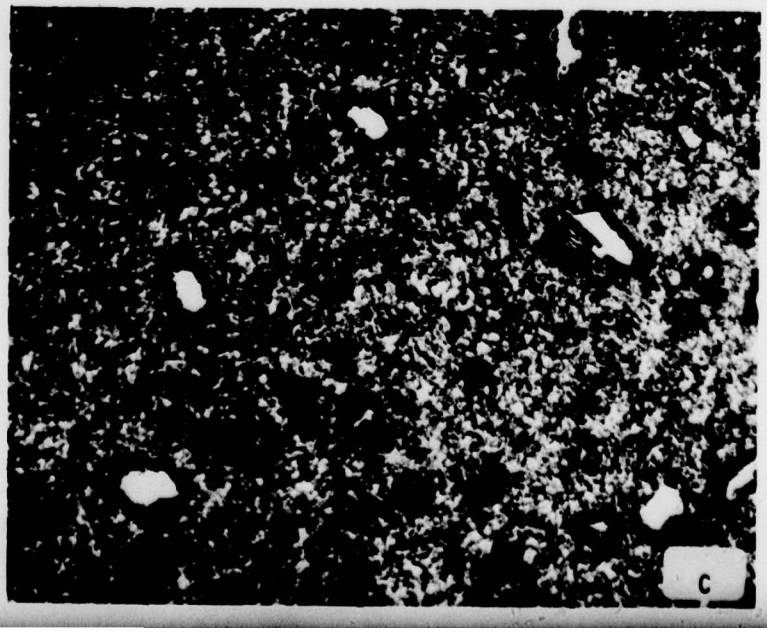
C

Fig. 7: Composite aluminium alloy containing 40-50% Vol. silicon carbide particles before and after being exposed to 500 gr. sand particles at 30^{o} impact angle. SEM examinations

A. Target surface before erosion showing the distribution size and concentration of silicon carbide particles.

B. Same area as in Fig. 7A showing one particle.

C. X-ray image of Si(Kα) showing the distribution of Si in 7B.

D. X-ray image of Al(Kα) showing the distribution of Al in 7B.

E. General appearance of target surface after being exposed to erosion conditions surface is characterized by cell or cratered type structure together with hard phase particles of silicon carbides.

F. Enlargement of the area shown in E. It reveals a single hard phase particle.

G. X-ray image of Si(Kα) in the area shown in F.

H. X-ray image of Al(Kα) in the area shown in F.


A


B


D

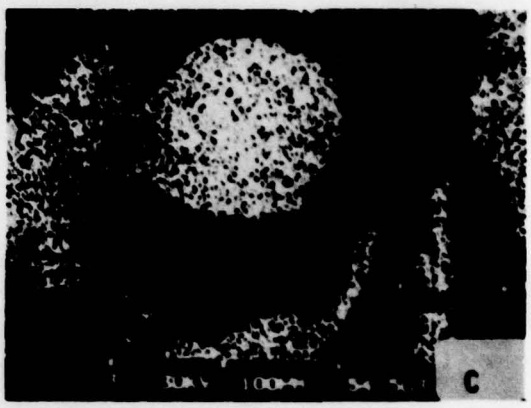
C


E

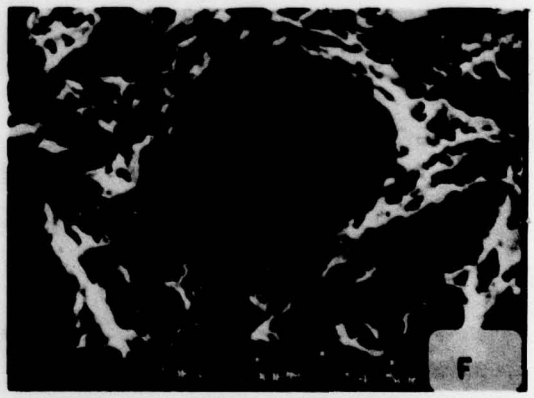
F


H


G

Fig. 8: Appearance of composite aluminium alloy containing 40-50% Vol. silicon carbide particles after being exposed to 500 gr. sand particles at various impact angles.

A. Eroded surface at impact angel of 30°, showing removal of silicon carbide particle from the surface.
B. X-ray image of Si(Kα) in the area shown in A.
C. Eroded surface at normal impact angle showing the removal of silicon carbide particle from the surface.
D. X-ray image of Si(Kα) in the area shown in C.
E. Eroded surface at normal impact angle showing the embedding of fragment of sand particle in the eroded surface.
F. X-ray image of Si(K) in the area shown in E.


1 30KV 30MM 54 507
A

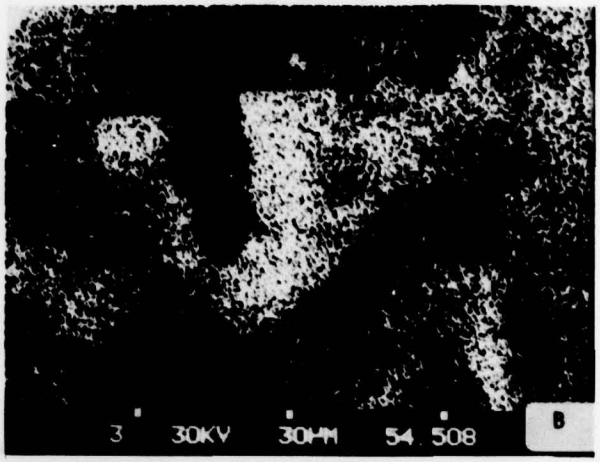
3 30KV 30MM 54 508
B

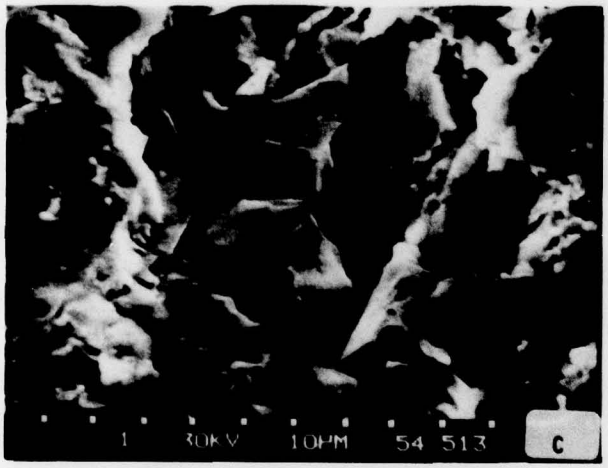
1 30KV 10MM 54 513
C

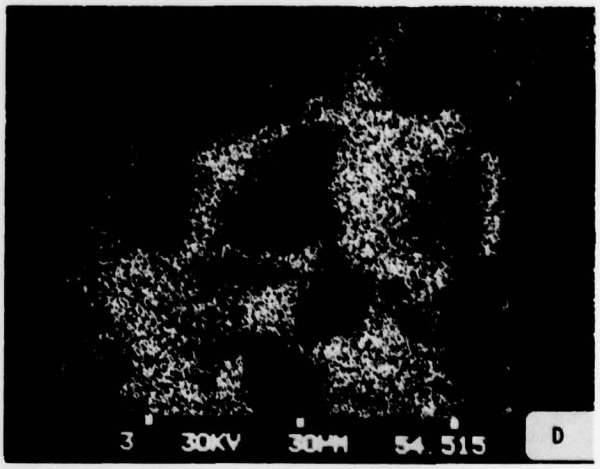
3 30KV 30MM 54 515
D


E


3 30KV 54 521
F

Fig. 9: Appearance of composite aluminium alloy containing 30% Vol. silicon carbide particles after being exposed to 500 gr. abrasive sand particles at various impact angles. SEM examinations

A. General view of eroded surface at impact angle of 30°. Cratered structure and particles are shown.

B. Enlargement of the area shown in A. A single eroded particle is shown.

C. X-ray image of Si(Kα) in the area shown in B.

D. Removal of material resulted in exposing a silicon carbide particle beneath the surface.

E. Removal of silicon carbide particle from a target surface exposed to impact angle of 60°.

F. X-ray image of Si(Kα) in the area shown in E.

G. Removal of silicon carbide particle from a target surface exposed to impact angle of 90°.

H. X-ray image of Si(Kα) in the area shown in G.

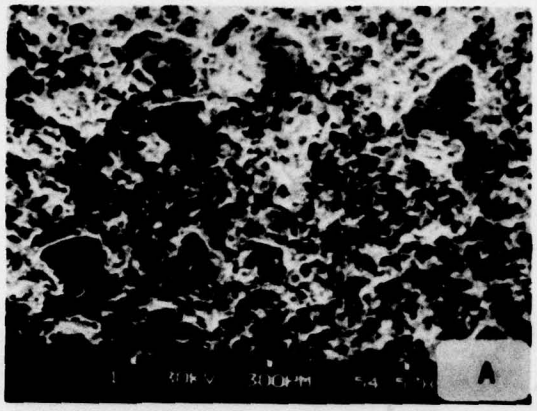
A


B

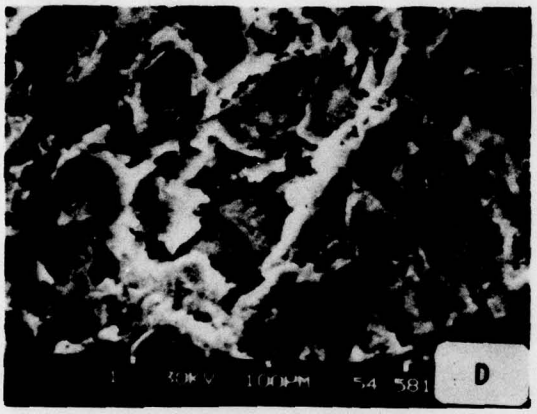
D

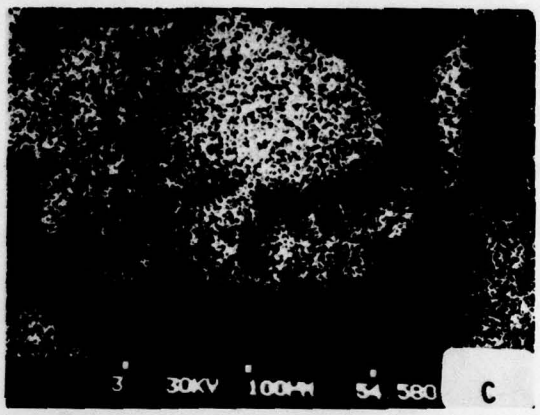
3 30KV 100µM 54 580
C

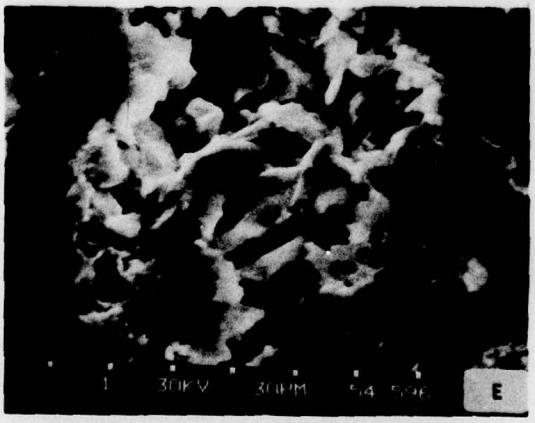
E

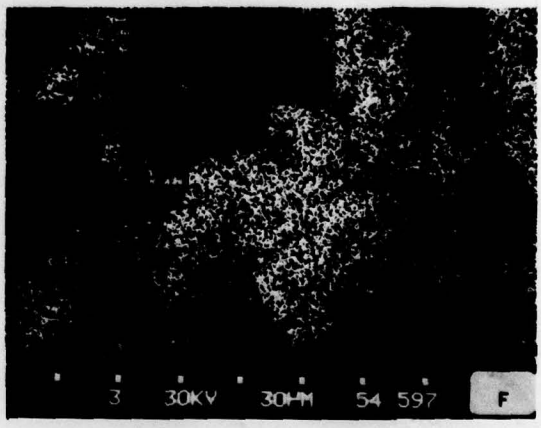
3 30KV 30µM 54 597
F

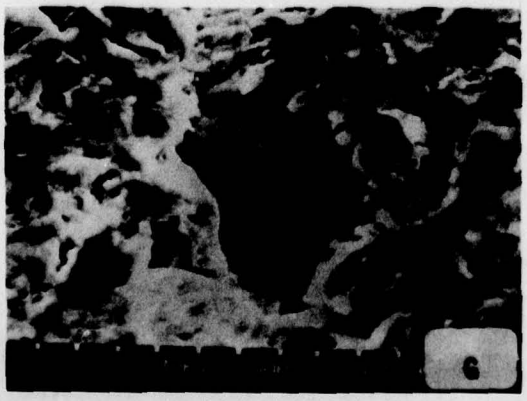
G


30KV 100µM
H

Fig. 10: Eroded surface appearance after being exposed to 500 gr. abrasive sand particle at impact angle of 30°. SEM examinations.

A. General view of eroded surface. Cell type or cratered structure together with particles are shown.

B. A typical single hard phase particle in the eroded area shown in A. Particle surfaces do not erode in the same way as the matrix.

C. X-ray image of Si(Kα) in the area shown in B indicating that the particle is actually SiC.

D. Removal of a hard phase silicon carbide particle from eroded surface which resulted in a fractured area.

E. Si(Kα) X-ray image showing the distribution of Si in area D indicating the presence of SiC.

F. Al(Kα) X-ray image for distribution of Al in area D.

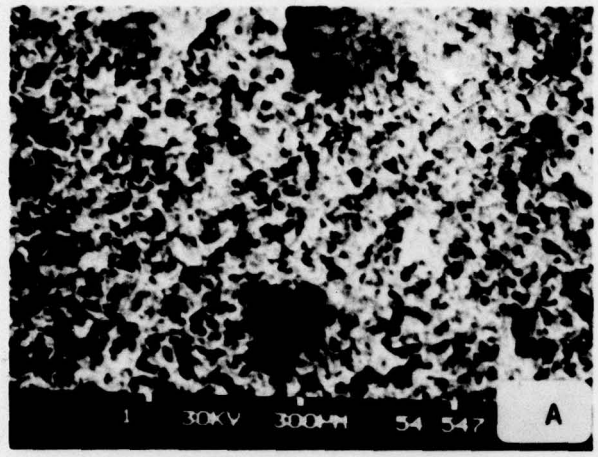
1 30KV 300HM 54 547
A

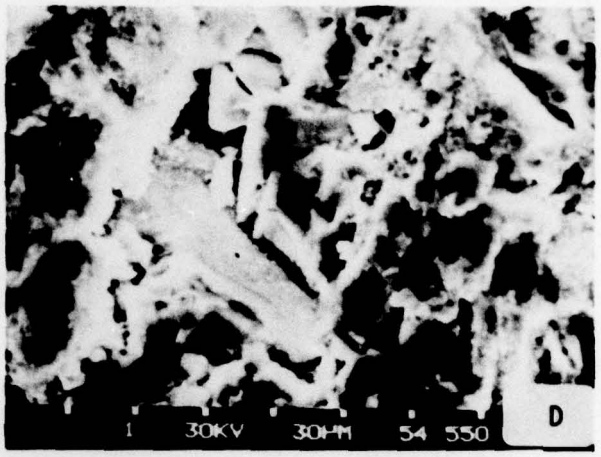
1 30KV 30HM 54 550
D

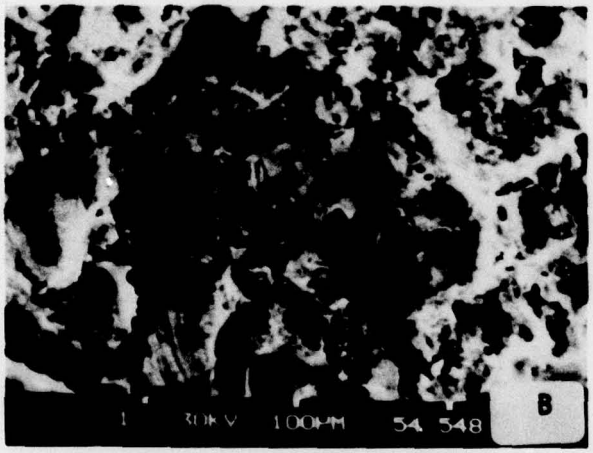
1 30KV 100HM 54 548
B


3 30KV 30HM 54 552
E

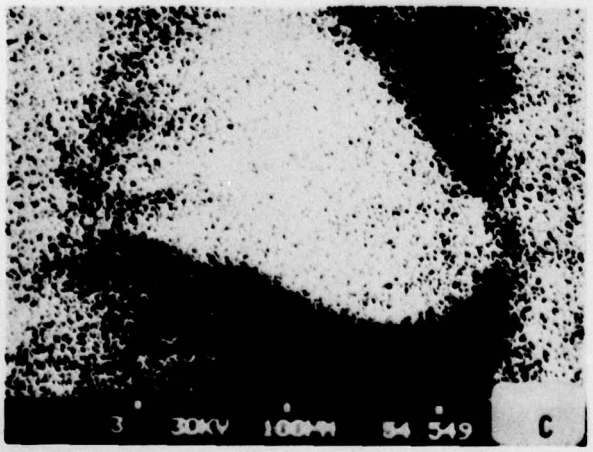
3 30KV 100HM 54 549
C

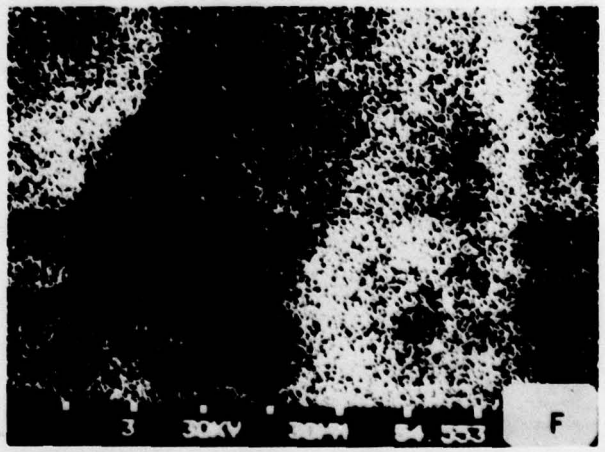
3 30KV 30HM 54 553
F

Fig. 11: Surface view of composite aluminium alloy containing 30% Vol. alumina particles before and after being exposed to erosion. SEM micrographs.

A. General appearance of target surface showing presence and distribution of alumina particles before erosion.

B. A typical alumina particle in the surface before erosion. It is noted that the alumina particles tend to aglomerate in local zones as shown also in A.

C. After erosion - presence of alumina particles in eroded surface exhibiting cell type or cratered structure. Target was subjected to 500 gr. sand particles at 30^{o} impingement angle.

D. High magnification view of area shown in C. Material removal and erosion process are shown around alumina particles.

E. After erosion - view of eroded target surface after being exposed to 500 gr. sand particles at 60^{o} impact angle. Presence of alumina particles within eroded cratered surface structure.

F. A typical view of erosion process or material removal in the vicinity of alumina particles in the eroded surface.

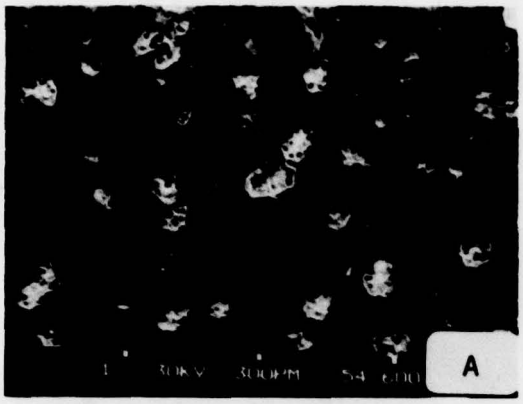
A

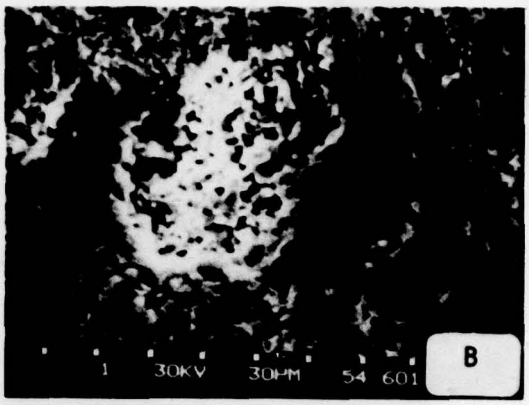
1 30KV 30µM 54 601
B


C

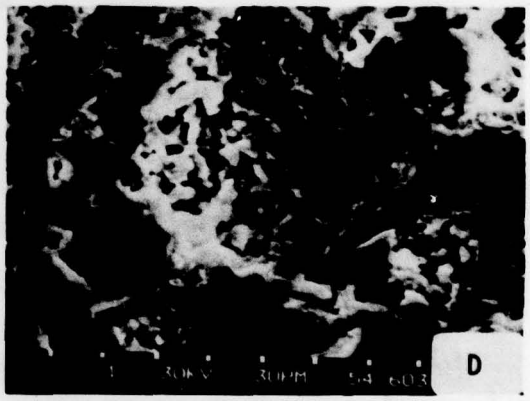
D


E

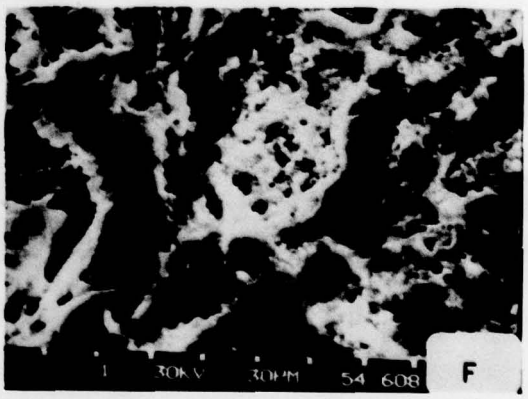
1 30KV 30µM 54 608
F

Fig. 12: Eroded surface of composite aluminium alloy containing 15% Vol. alumina particles after being exposed to 500 gr. abrasive sand particles at various impact angles.

A. Eroded surface impacted at 30^{o}. Cell type structure and some alumina particles are shown.

B. A typical alumina particle within the eroded area characterized by cell structure. Magnification of the area shown in A.

C. Eroded surface impacted at 60^{o} resulted in cell type structure. Also some alumina particles are shown within the eroded surface.

D. Detailed eroded surface structure of the area shown in C.

E. Eroded surface impacted at 90^{o} resulted in cell type structure which is characteristic also of non-composite alloys.

F. Detailed structure of the eroded area shown in Fig. E.

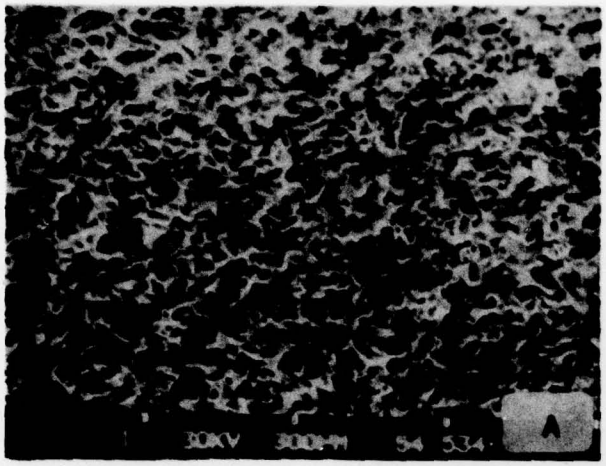
1 30KV 300HM 54 534
A

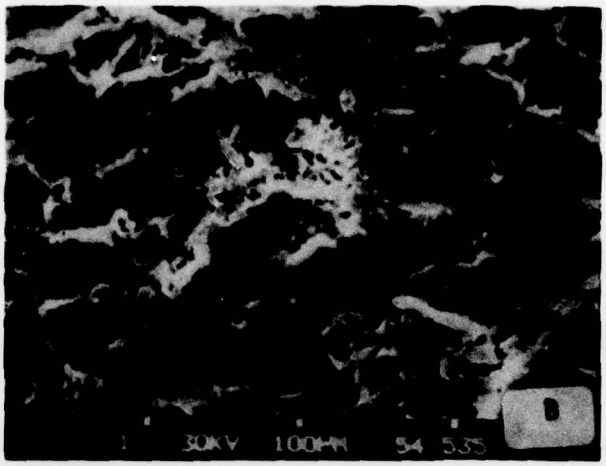
1 30KV 100HM 54 535
B


C

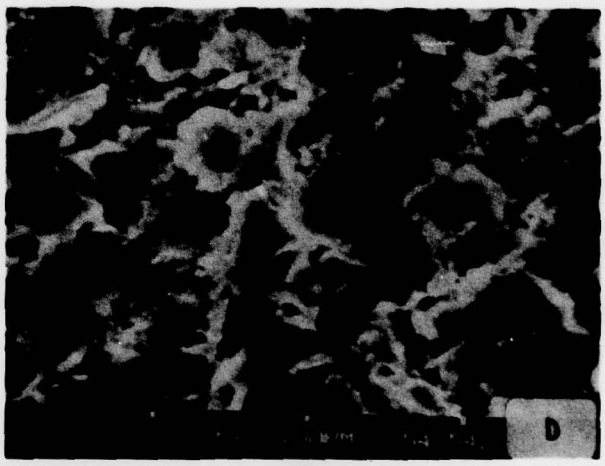
D

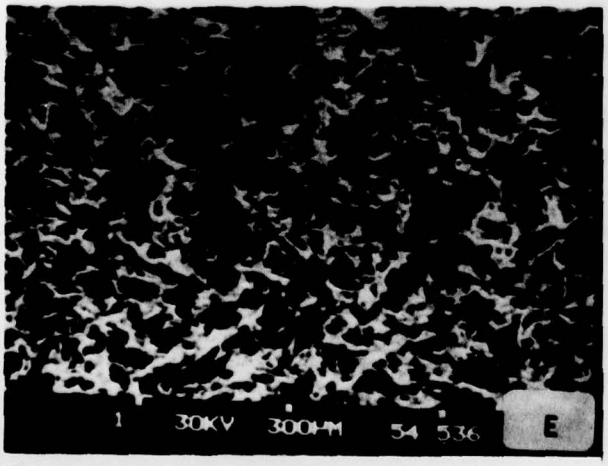
1 30KV 300HM 54 536
E


1 30KV 100HM 54 53
F